

ANNALS OF THE NEW YORK ACADEMY OF SCIENCES

Issue: *Evolutionary Dynamics and Information Hierarchies in Biological Systems***Establishing epigenetic domains via chromatin-bound histone modifiers**

Fabian Erdel, Katharina Müller-Ott, and Karsten Rippe

Deutsches Krebsforschungszentrum (DKFZ) and BioQuant, Research Group Genome Organization & Function, Im Neuenheimer Feld 280, Heidelberg, Germany

Address for correspondence: Karsten Rippe, Deutsches Krebsforschungszentrum, Research Group Genome Organization & Function (B066), Im Neuenheimer Feld 280, 69120 Heidelberg, Germany. Karsten.Rippe@dkfz.de

The eukaryotic nucleus harbors the DNA genome, which associates with histones and other chromosomal proteins into a complex referred to as chromatin. It provides an additional layer of so-called epigenetic information via histone modifications and DNA methylation on top of the DNA sequence that determines the cell's active gene expression program. The nucleus is devoid of internal organelles separated by membranes. Thus, free diffusive transport of proteins and RNA can occur throughout the space accessible for a given macromolecule. At the same time, chromatin is partitioned into different specialized structures such as nucleoli, chromosome territories, and heterochromatin domains that serve distinct functions. Here, we address the question of how the activity of chromatin-modifying enzymes is confined to chromatin subcompartments. We discuss mechanisms for establishing activity gradients of diffusive chromatin-modifying enzymes that could give rise to distinct chromatin domains within the cell nucleus. Interestingly, such gradients might directly result from immobilization of the enzymes on the flexible chromatin chain. Thus, locus-specific tethering of these enzymes to chromatin could have the potential to establish, maintain, or modulate epigenetic patterns of characteristic domain size.

Keywords: histone modifications; chromatin looping; pattern formation; epigenetics; nuclear organization

Introduction

The genomic DNA of eukaryotes is organized into linear chromosomes with several tens or hundreds of million base pairs (bp) of DNA that is packaged by interactions with histones and other proteins into chromatin. The building block of chromatin is the nucleosome, a complex of a histone octamer that associates with 145–147 bp of DNA wrapped in almost two turns around the octamer. The genome is confined by the nuclear envelope to the cell nucleus. Within the nucleus, no membrane-separated organelles exist. Thus, molecules are free to diffuse within the accessible space. Since diffusion equilibrates concentration gradients, one would expect that all places connected by diffusive transport are equivalent with respect to their molecular composition and function. This is clearly not true for the organization of the genome within the nucleus. Rather, chromatin is organized into functionally

and structurally distinct nuclear subcompartments such as nucleoli, chromosome territories, regions of denser heterochromatin, or more open and frequently more active euchromatin. The associated chromatin states differ with respect to their protein content, nucleosome spacing and positioning, DNA methylation, and histone modifications, as well as the presence of chromatin-associated RNAs. In this manner, access to the DNA for the selection of the active gene-expression program and other genome functions such as DNA replication and repair is controlled (Fig. 1A).

In the presence of freely diffusive enzymes at constant concentrations throughout the nucleus, every nucleosome would have essentially the same probability of colliding productively with an enzyme that could modify it. Modification reactions are characterized by the addition or removal of small chemical groups, such as methyl, acetyl, or phosphate groups, at one of the histone tails or the

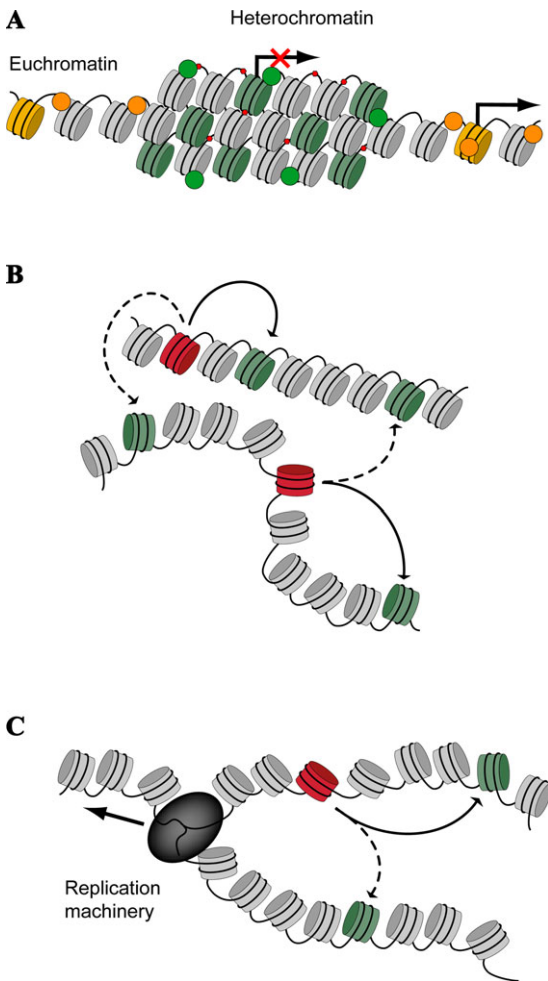


Figure 1. Chromatin states and their propagation. (A) Chromatin is organized into different chromatin states that in a simplified classification are referred to as denser and transcriptionally silenced heterochromatin versus the more open and biologically active euchromatin. The states are different with respect to specific DNA and histone modifications as well as protein composition. In the scheme, DNA methylation is depicted by red circles, nucleosomes with repressive histone modifications such as H3K9me3 or H3K27me3 are shown in green, and nucleosomes with activating modifications (e.g., H3K4me3, H3K36me3) are colored in orange. In addition, bound chromosomal proteins that are associated with the two chromatin states are represented by orange and green circles. (B) Histone modifications can be propagated from nucleation sites to form epigenetic chromatin domains. (C) During DNA replication, nucleosome modifications are lost as new histones are incorporated. This dilution of histone modification patterns behind the replication fork has to be compensated for by propagating the original modification state to the newly formed nucleosomes.

histone core. However, there are several ways to establish heterogeneous chromatin-state patterns in the nucleus: (1) diffusion might be slow as compared to processes that actively create gradients, (2) external boundaries (e.g., the nuclear envelope) can impose mobility constraints that depend on the distance to a given boundary, and (3) a heterogeneous distribution of enzymes that is not balanced by diffusion can result from the binding of enzymes to a less-mobile chromatin scaffold.

Here, we consider different mechanisms for the formation of chromatin subcompartments within the cell nucleus. Although most enzymes that establish such patterns are small enough to move through the whole nucleus, their distribution is not necessarily homogeneous since they can bind to a heterogeneous chromatin network. A direct consequence might be the generation of activity gradients that follow their net abundance. These can lead to the formation of chromatin patterns and thus, partition chromatin into distinct domains.

Epigenetic chromatin states

Historically, chromatin has been globally classified on the basis of the chromatin density distribution in microscopy images into more compact biologically inactive heterochromatin and transcriptionally active euchromatin.^{1,2} Transitions between these two states at some chromosomes were accounted for by the introduction of the term *facultative heterochromatin*. One example of this transition is the inactivation of one X chromosome in female mammalian cells, in which one X chromosome adopts a distinct silenced conformation state termed as the Barr body while genes on the other X chromosome are transcriptionally active. Other functionally distinct regions include chromatin at the centromeres,^{3,4} pericentromeric heterochromatin,^{5,6} chromatin at the nuclear lamina, telomeric chromatin,^{7,8} and active and repressive ribosomal genes in nucleolar chromatin.⁹

More recently, systematic chromatin maps have been acquired that evaluate either the protein composition, DNA methylation, or posttranslationally incorporated histone modification patterns such as acetylation, methylation, or phosphorylation to identify structurally and functionally distinct chromatin states.^{10–12} These include (1) the identification of five major chromatin states greater than 100 kb in length in *Drosophila*,¹⁰ (2) the

categorization of 18 different histone acetylation or methylation marks into nine patterns to characterize functional genomic elements in *Drosophila*,¹¹ and (3) the evaluation of two histone acetylation marks, six histone methylation modifications, and binding of CCCTC binding factor (CTCF) in different human cell types to identify chromatin patterns that characterize their cell type-specific gene expression profiles.¹²

The functional consequences of establishing a certain chromatin state can be related to changes in DNA accessibility for interacting factors. These can be brought about by different mechanisms. For some modifications such as the acetylation of histones at certain positions (e.g., H4K16ac, H3K56ac, H3K64ac, H3K122ac), there appears to be a direct effect on nucleosome–nucleosome interactions and stability.^{13–18} Other modifications enhance the binding of architectural chromatin components that can recognize certain modifications such as methyl-CpG-binding protein MeCP2 for DNA methylation¹⁹ or heterochromatin protein 1 (HP1) for the trimethylation of histone H3 at lysine 9 (H3K9me3) to change chromatin organization.²⁰ An additional important parameter of the local chromatin structure is the positioning of nucleosomes. These separate the nucleosomal DNA that interacts with histone proteins from the linker DNA between nucleosomes, which is more accessible to soluble factors. This accessibility pattern is tightly linked to histone and DNA modifications as well as other chromatin features.²¹ It is functionally important since DNA-dependent processes such as transcription require the binding of enzymes to the DNA. In many instances, binding of transcription factors to nucleosomal DNA is impeded.²²

Some of the fundamental questions regarding the setting of the cell's active gene expression program by establishing a specific pattern of chromatin states currently remain unanswered: How are chromatin-modifying enzymes targeted to or excluded from chromatin in a spatially defined manner? Once a given nucleosome modification is established, how can it be propagated on the same or different nucleosomes to establish a specific chromatin domain (Fig. 1B)? How is this state reestablished or maintained during DNA replication (Fig. 1C)? Since most enzymes that catalyze DNA and histone modifications are small, they can diffuse rapidly through the nucleus and could potentially modify every nu-

cleosome with which they collide. Thus, spatially heterogeneous epigenetic patterns are established in the context of a well-mixed nucleus. In the following sections, we discuss different possibilities to generate spatially confined chromatin patterns. In particular, we consider the case that chromatin-bound enzymes can give rise to local activity gradients, which appears to be a simple and robust way to establish and maintain epigenetic patterns.

Interactions between genomic loci owing to chromatin dynamics

The contour length of the DNA of one mammalian chromosome is in the order of tens of centimeters, whereas the diameter of the cell nucleus is only 10–20 μm . Thus, DNA packaged into chromatin is highly compacted in the nucleus. Both DNA and the nucleosome chain can be described as polymer chains.^{23,24} Individual chromosomes occupy distinct territories during interphase.²⁵ They have a large friction coefficient and translocate only slowly over micrometer distances within minutes and hours.²⁶ In contrast, small chromatin domains translocate significantly on length scales of tens to hundreds of nanometers within milliseconds to seconds due to diffusion.²⁶ Thus, individual segments of the chromatin chain can jiggle around their equilibrium position more rapidly, that is, make small displacements within a local confinement region. This confined diffusive motion of chromatin loci can be directly visualized using different microscopy techniques.^{27–29} Motion of chromatin segments within the dense chromatin network leads to collisions, and nucleosomes located on the segments are able to contact each other. This is both true for nucleosomes on the same chromosome and nucleosomes on different chromosomes, with intrachromosomal collisions making the dominant contribution in genome-wide interaction maps (Fig. 1B).³⁰

The inherent properties of the chromatin chain define two intrinsic length scales that are relevant for intra- and interchromosomal interactions. The first length scale reflects the flexibility and the conformation of the nucleosome chain. It determines the local concentration profile for nucleosomes on the same chromosome, as discussed in further detail below. This scale dictates the probability for the chain to fold back on itself and thus for local intrachromosomal interactions to occur. The second scale is

the confinement radius that restricts the diffusive motion of a chromatin locus in three-dimensional (3D) space. This scale is relevant for interactions that occur between nucleosomes that are in spatial proximity, independent of their genomic coordinate (i.e., their separation distance along the chromosome) and independent of whether they are located on the same chromosome. Measurements of intrachromosomal collision frequencies suggest that intrachromosomal collisions occur efficiently within distances of around 2–4 kb,^{31–33} which corresponds to a contour length of several hundred nanometers of the nucleosome chain (Fig. 2). Microscopy experiments with labeled nucleosomes or chromatin loci reveal that the diffusive confinement radius is on a similar length scale of 100–300 nm.^{27–29} This fits well with the size of ~1 Mb topological domains containing ~5000 nucleosomes that have been identified using the chromosome conformation capture (3C) method^{30,34} as well as microscopy-based techniques.²⁶ Thus, the natural domain size of chromatin might be intimately related to the restricted mobility of chromatin loci, and raises the possibility that the formation of epigenetic domains relies on diffusion-driven mechanisms.

Calculating the contact probability between nucleosomes within the chromatin chain

To make quantitative statements about nucleosome–nucleosome interaction probabilities, polymer models can be applied that are based on either a freely jointed chain^{35–37} or a worm-like chain.^{38–40} With these theoretical descriptions, the stiffness of a nucleosome chain is described by the statistical segment length or Kuhn length (l) or the persistence length (a), which is related to the Kuhn length according to $l = 2a$. The numerical value of l increases with the stiffness of the polymer. The interaction probability between two sites on the same chain is expressed as the molar local concentration (j_M) of one locus in the proximity of the other.^{23,24} The value of j_M is equivalent to the concentration that would be required free in solution to obtain the same contact probability. If a given site is bound by a protein, the same applies for the respective protein concentration. In this case, the occupancy (θ) of the protein-binding site, as well as the interactions with the proteins not bound to the DNA, needs to be considered. In the

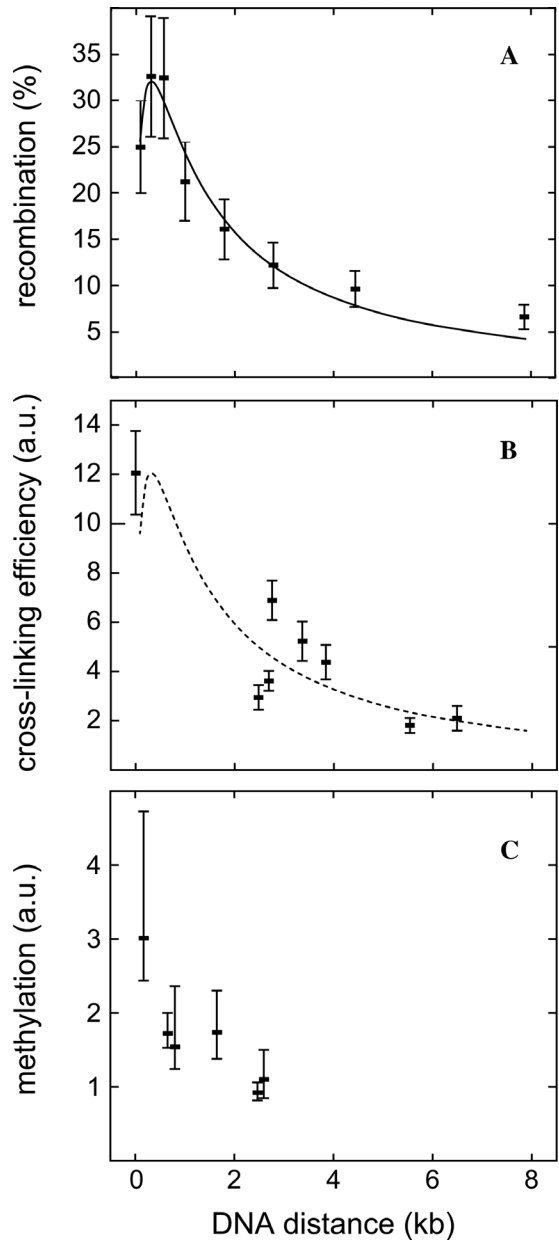


Figure 2. Experimentally measured short-range intrachromosomal interactions. (A) Contact probabilities between two sites on the same chromosome in a human cell line measured by FLP recombination frequency in Ref. 32. The solid line is the least-squared fit to Eq. (3) including some baseline offset and scaling factor. The fit yields $m_b = 160$ bp and $d = 0.16$. (B) Cross-linking efficiency from a 3C experiment.³³ (C) Dependence of *dam* methylation level on the distance of an immobilized *dam* methyltransferase.³¹

balance of this presentation, we assume that the occupancy of the binding site is unity, that is, the interacting site is always fully occupied and c_{free} , the concentration of protein not bound to the DNA, is much smaller than j_M . Under these conditions c_{eff} , the effective protein concentration, is equal to j_M . If this is not the case, c_{eff} can be calculated according to Eq. 1

$$c_{\text{eff}} = \theta \times j_M + c_{\text{free}}. \quad (1)$$

As described previously,^{23,24} j_M between two sites at a distance of n segments of length l on a linear polymer can be calculated according to

$$j_M(n) = 0.53 \times n^{-\frac{3}{2}} \times \exp\left(\frac{d-2}{n^2+d}\right) \times l^{-3} \frac{\text{mol} \cdot \text{nm}^3}{\text{liter}}. \quad (2)$$

The additional parameter d incorporated into Eq. 2 reduces the contribution of the exponential term if d is larger than zero. This can account for an increase of j_M at short separation distances ($n < 4$), for example, due to the size of interacting protein complexes or if intrinsic DNA curvature is present.^{24,41} In this general form, the local molar concentration j_M of one site in the proximity of the other site is given per l^3 , that is, with units mol·nm³/liter. In Eq. 2, the separation distance n between two sites is given as a dimensionless reduced separation distance, which is simply the number of Kuhn segments with length l that corresponds to the site-separation distance. Thus, the expression in Eq. 2 is independent of the characteristics of a specific polymer and has a maximum of $n = 1.6$ for $d = 0$.

For DNA-mediated interactions, it is convenient to express the site-separation distance n by the number of DNA base pairs b . With n_b being the number of DNA base pairs per segment length, this yields Eq. 3:

$$j_M(b) = 0.53 \times \left(\frac{b}{n_b}\right)^{-\frac{3}{2}} \times \exp\left(\frac{d-2}{\left(\frac{b}{n_b}\right)^2 + d}\right) \times l^{-3} \frac{\text{mol} \cdot \text{nm}^3}{\text{liter}}. \quad (3)$$

In order to compute j_M from Eq. 3, we need to know the stiffness and contour length of the chain

to be able to express n_b . So far no consensus has been reached from experimental measurements for either the stiffness of the nucleosome chain or for its contour length. If expressed in nanometers, both parameters would be highly dependent on the folding of the chain.^{42,43} It appears that the short length regime of <10 kb has to be treated separately from long-range interactions at sites 10–500 kb apart. At short separation distances, the interaction probability is likely to reflect the nucleosomal organization of the chain more resembling free double-stranded DNA with intrinsically curved regions due to wrapping of DNA around the histone octamer, and possibly further compaction due to interactions between nucleosomes. Thus, the characteristic contour length of the nucleosome chain per base pair of DNA is very different from that of free DNA, for which a value of 0.34 nm/bp is well accepted.

For the long-range interactions, the higher order organization of chromatin into transient or stable loops of different sizes needs to be included into the polymer model through different stiffness and contour-length parameters.^{24,26} Here we focus on the short-range interactions between nucleosomes at distances <10 kb. In general, these appear to be orders of magnitude more frequent than interactions on the 100 kb scale and above, as apparent from 3C experiments that measure both short- and long-range interactions.³⁰ The experimentally determined short-range intrachromosomal interaction probabilities from three different types of experiments are plotted in Figure 2. Notably, the contact frequencies between two sites on the same chromosome measured by (1) the DNA recombination frequency mediated by the flippase (FLP) enzyme³² (Fig. 2A), (2) the cross-linking efficiency from 3C experiments³³ (Fig. 2B), and (3) the levels of ectopic adenine methylation around an immobilized *dam* methyltransferase³¹ (Fig. 2C) yield very similar distance dependencies for the interaction between two separated sites on the same chromosome. Interactions occur most frequently within <1 kb separation distance and decay to base line levels above ~5 kb. These conclusions are further supported by *in vitro* experiments with reconstituted nucleosomal arrays and theoretical studies that showed highly efficient enhancer–promoter interactions at separation distances between 0.7 and 4.5 kb.⁴⁴

As the data for FLP recombination frequency were acquired in living mammalian cells at high resolution, they provide an excellent reference for computing j_M independent of the base pair–separation distance. A similar approach was already used in Ref. 32, but with a chain contour length for free DNA. Here, we estimate the contour of an unfolded nucleosome chain from simple geometric considerations as follows. The nucleosome repeat length (i.e., the length of DNA in a nucleosome plus linker DNA) equals roughly 190 bp (e.g., Ref. 22 measured 191 bp for mouse cells). The well-established value of 145–147 bp of nucleosomal DNA results in a linker of 45 bp or 15.3 nm DNA between two nucleosomes. Since the distance between the entry–exit site in the nucleosome is about 9 nm,⁴⁵ a contour length of 24.3 nm/191 bp or 0.13 nm/bp is obtained. With these values, a fit of the FLP recombination data yields Eq. 4 with $n_b = 160$ bp, $d = 0.16$, and $l = 160$ bp·0.13 nm/bp = 21 nm, for computing the local concentration j_M in mol/liter of a nucleosome in the close proximity of another nucleosome separated by b base pairs on the same chain.

$$j_M(b) = 5.7 \times 10^{-5} \times \left(\frac{b}{160}\right)^{-\frac{3}{2}} \times \exp\left(\frac{-1.84}{\left(\frac{b}{160}\right)^2 + 0.16}\right) \frac{\text{mol}}{\text{liter}}. \quad (4)$$

The above description considers the equilibrium distribution for interactions between nucleosomes on the same chain as represented by their local concentrations. The kinetics with which these interactions occur can be estimated from studies of DNA contacts for separation distances of ~ 10 nm, which corresponds to the length of the linker between nucleosomes. From Brownian dynamics simulations of DNA molecules, collision frequencies of roughly 1000/s were derived.⁴¹ This value fits well with the experimentally determined rates for loop closure of similar-sized DNA hairpins.⁴⁶ Furthermore, even much larger chromatin domains show translocations on the 10 and 100 nm length scales in living cells within the 30–50 ms time resolution of the measurements.^{27,28} Thus, looping-mediated interactions between nucleosomes occur on the time scale of milliseconds.

Normalization of experimentally measured interaction probabilities

While Eq. 3 is generally applicable for computing interaction probabilities, specific stiffness and contour length parameters of the chain are required to derive the local concentration in molar units. Since there is an ongoing dispute in the field on how to best choose these parameters for chromatin, we introduce a complementary approach to estimate the scaling of the j -function for chromatin looping. We consider a single chromosome residing in its territorial space during interphase of the cell cycle. Accordingly, the vast majority of interactions between nucleosomes are intramolecular. This description can be easily extended to the complete genome by considering the nucleus as being filled by a set of chromosomes that occupy distinct spatial territories.^{25,26,47}

The local concentration function ($j(n)$) is proportional to the probability ($p(n)$) that a given nucleosome resides within a volume element (dV) around the same chromosome that is separated by distance n along the chain (Fig. 3A). The volume element dV can be described as a cylinder with height dn and radius r , which is chosen as sufficiently small to ensure that the local nucleosome concentration within the volume element is approximately constant. Thus, the average local concentration ($\langle j \rangle$) of a given nucleosome within a tube with radius r around the whole chromosome can be expressed as

$$\langle j \rangle = \frac{2}{L} \int_0^{L/2} j(n) dn = \frac{1}{L \pi r^2} = \frac{1}{V_{\text{chr}}}. \quad (5)$$

Here, L is the contour length of the chromosome and $V_{\text{chr}} = L \pi r^2$ is the volume of the tube surrounding the chromosome, which can be regarded as the volume occupied by the chromosome. For simplicity, the nucleosome at the center of the chromosome was considered for Eq. 5, yielding equal local concentrations to the left and right of the nucleosome. This is a good approximation for all nucleosomes, since mammalian chromosomes have a length of 10–100 Mb while the j -functions considered here have a typical width of several thousand base pairs. Using the definition of the average nucleosome concentration $c_{\text{nuc}} = N_{\text{nuc}}/V_{\text{CT}}$, with N_{nuc} being the total number of nucleosomes in the territory with volume V_{CT} ,

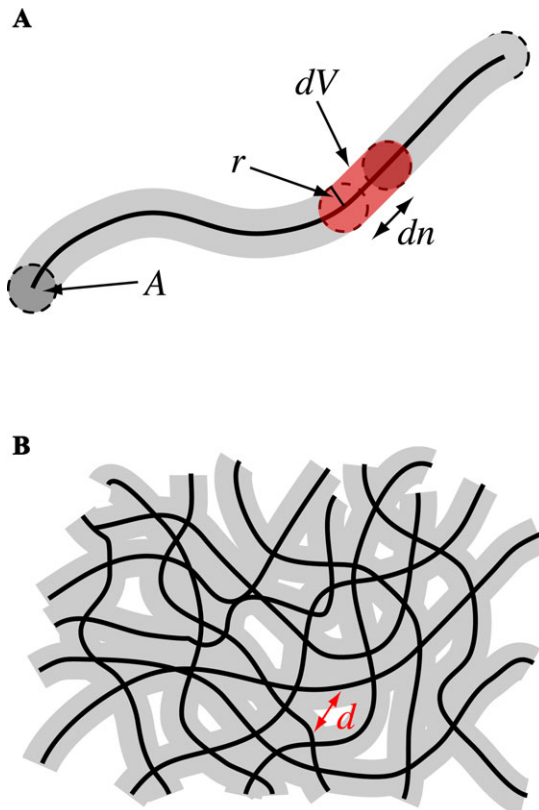


Figure 3. Conversion of interaction probabilities to local concentrations. Experimentally determined contact probabilities can be converted into local concentrations for tightly packed chromatin as found in the cell by normalization to the average nucleosome concentration. (A) The local concentration determines the probability at which a nucleosome may be present in a small volume element dV (red) separated by a given distance along the chromosome. (B) A part of a chromosome territory is depicted. Since chromosomes are tightly packed, the volume of the territory can be similar to the volume of a tube around the chromosome (gray), which has a radius r that is similar to the size of a nucleosome.

Eq. 5 can be rewritten as

$$\langle j \rangle = \frac{1}{V_{\text{chr}}} = \frac{V_{\text{CT}}}{V_{\text{chr}}} \frac{c_{\text{nuc}}}{N_{\text{nuc}}} \geq \frac{c_{\text{nuc}}}{N_{\text{nuc}}}. \quad (6)$$

Here, the inequality sign accounts for the fact that a chromosome cannot occupy more space than available in its territory. For a tightly packed chromosome, the two volumes might be similar (i.e., $V_{\text{chr}} \approx V_{\text{CT}}$). At the average nucleosome concentration $c_{\text{nuc}} = 140 \mu\text{M}$ measured in a human cell line,⁴⁸ the average distance between neighboring nucleosomes corresponds to less than 40 nm if

a random distribution is assumed (Fig. 3B). Thus, the local nucleosome concentration would be approximately constant over the separation distance between neighboring nucleosomes, and the radius r of the chain could be chosen accordingly to ensure that $V_{\text{chr}} \approx V_{\text{CT}}$. In this case, the average local concentration $\langle j \rangle$ equals the concentration of a nucleosome in the territory $1/V_{\text{CT}}$, and Eq. 6 simplifies to

$$N_{\text{nuc}} \langle j \rangle \approx c_{\text{nuc}}. \quad (7)$$

Thus, Eqs. 6 and 7 provide normalization conditions that are imposed by the constant number of nucleosomes N_{nuc} within the chromosome territory. They can be computed by either integrating the average nucleosome concentration over the nuclear volume or by integrating the local concentration of all nucleosomes over the volume occupied by the chromosome. If one considers j to be proportional to a residence time, Eqs. 6 and 7 mean that a nucleosome spends all its time within the chromosome territory and that its residence times at all the positions it samples add up to this time. Since Eq. 4 is consistent with the normalization according to Eqs. 6 and 7, we conclude that it is justified to use a polymer model with the given parameter set to compute j . With Eqs. 6 and 7 it is possible to estimate absolute concentrations from arbitrary contact probability functions without using a particular polymer model for the description of the nucleosome chain. However, the volume that is occupied by the nucleosome chain has to be estimated carefully. Nonetheless, we feel that the concept described in this section might prove useful for calculating concentrations from experimentally determined interaction maps provided by different methods such as the ones described in the following sections.

Mechanisms for establishing gradients of enzymatic activity

There are several ways to establish gradients in living organisms in the presence of counteracting diffusive mixing. The most straightforward option is a source–sink mechanism, in which a component is rapidly released at one location and rapidly removed at another location. If release and removal are fast compared to the time the components need to diffuse between both locations, a gradient is established. The source–sink model has been discussed extensively in the context of morphogenic gradients

during embryogenesis.^{49–51} However, for steep intracellular gradients with small spatial extension, this mechanism is inefficient since very high release and removal rates would be needed to counteract diffusion, which is very fast on small length scales. Particles of the size of typical chromatin enzymes require roughly 1 s to diffuse through the whole cell nucleus (i.e., release) and removal processes would have to occur on the millisecond time scale. Although transient intracellular gradients might be established by such a mechanism (e.g., by triggered nuclear import of a protein), it would consume much energy to maintain steep gradients through constitutive pumping.

Another possibility for the establishment of gradients or patterns of enzymatic activity is through binding of the enzyme to a scaffold. In the nucleus, this can be achieved by tethering enzymes to the nuclear membrane or to chromatin (Fig. 4). Since chromatin fibers exhibit confined diffusion (i.e., they jiggle around their equilibrium position but do not make large translocations most of the time), binding of an enzyme to a chromatin locus increases the local enzyme concentration in the vicinity of the locus. Similarly, proteins attached to the nuclear envelope might diffuse laterally but do not make large radial translocations, since the radial position of the membrane is fixed by the nuclear lamina (Fig. 4A). Thus, a steep radial gradient can easily be established by tethering an enzyme to the nuclear envelope. The spatial distribution of an enzyme might directly translate into a distribution of enzymatic activity if the enzyme is active in the bound state. A well-studied example for such a case is the immobilization of regulator of chromosome condensation 1 (RCC1) on mitotic chromosomes⁵² (Fig. 4B). RCC1 serves as guanine nucleotide-exchange factor for the small GTPase Ran. RCC1 is even more active in the chromatin-bound state,⁵³ which leads to enhanced production and release of Ran–GTP (guanosine triphosphate) at mitotic chromosomes. Although Ran–GTP can quickly diffuse away from the chromosomes, which would ultimately result in a uniform Ran–GTP distribution, a constitutive gradient is achieved since Ran–GTP has a half-life that is shorter than the respective diffusion time.^{54,55} Consequently, Ran–GTP quickly converts into Ran–GDP (guanosine diphosphate) after having detached from chromatin, leading to increased Ran–GTP levels around

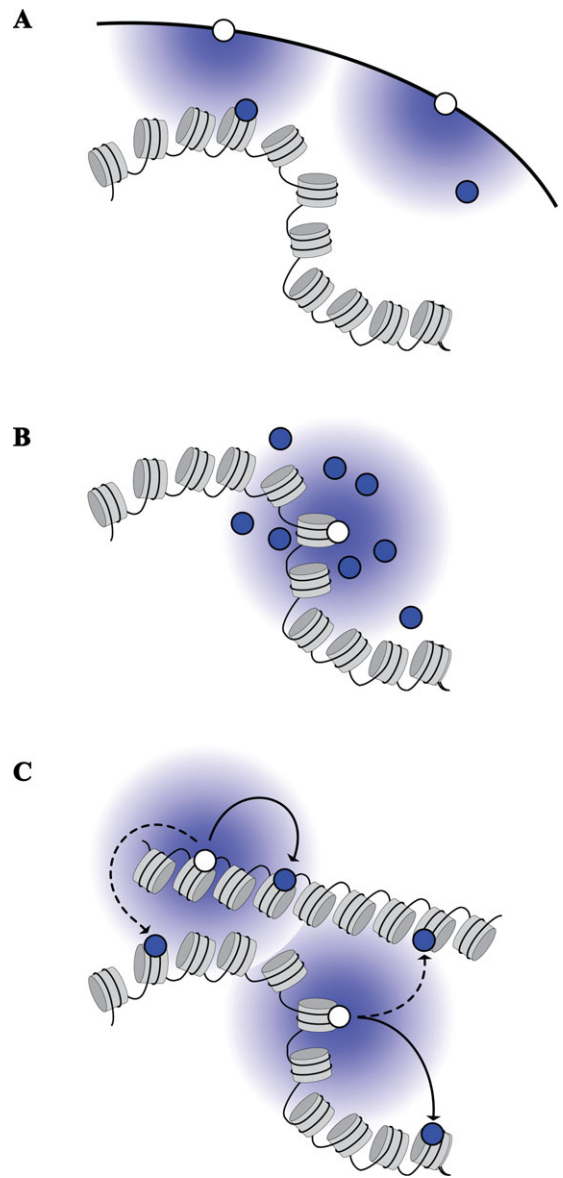


Figure 4. Pattern-formation mechanisms involving immobilized enzymes. Patterns or gradients within the cell nucleus can be established by different mechanisms: (A) Binding of enzymes (white circles) at the nuclear membrane where they continuously catalyze reactions to generate products (blue circles). (B) Binding of enzymes to the nucleosome chain, which produces compounds that diffuse away until they decay. (C) Binding of chromatin-modifying enzymes to the nucleosome chain, which can interact with neighboring nucleosomes to modify them via looping-mediated interactions to establish a specific pattern of epigenetic modifications around the binding site.

chromosomes. In this manner, a persistent Ran–GTP gradient is established around chromatin-bound RCC1.

Other chromatin-bound enzymes could establish similar gradients and patterns. Enzymes that are bound to chromatin and at the same time use chromatin as their substrate might establish distinct chromatin states around their binding sites (Fig. 4C). For patterns of soluble substrates, it is important to provide an efficient depletion mechanism, which would be the short half-life in the case of Ran–GTP. This is not required if chromatin is the substrate, since nucleosomes exhibit only confined diffusion and thus cannot balance concentration gradients of a nucleosomal species on biologically relevant time scales. If an enzyme immobilized on the chromatin fiber is able to productively collide with adjacent substrate nucleosomes as described in the previous section, this would immediately give rise to a higher concentration of enzymatic activity in the vicinity and thus to an enrichment of modified nucleosomes. In this scenario, the size of such a domain around the immobilized enzyme is strongly influenced by the flexibility of the chromatin chain. The folding and compaction state of the fiber could result in a modulation of domain size. With respect to setting DNA or histone modifications by a stably chromatin-bound enzyme that catalyzes the corresponding reaction, several predictions can be made. First, the chromatin modification is established locally around a nucleation region if the free concentration of the catalytically active form of the nucleated enzyme is comparably small with respect to the local concentration due to chromatin looping. Otherwise, the effect would no longer be localized, since the reaction would also be catalyzed at other sites by the freely mobile enzyme. Second, the typical spreading distance is determined by the diffusive motion of the nucleation region as well as the concentration (and productivity) of the free enzymes. For typical values, domain sizes of less than 10 kb are expected. Third, no boundary factors are required to limit the spreading of the modifications, since the diffusive motion of the bound enzyme is inherently confined. Fourth, modified chromatin regions have spherical shapes since there is no preferred direction for diffusive motion. And fifth, the steady-state modification level is not bistable unless nucleation sites are coupled in a complex manner via feedback loops.

Although it is difficult to directly demonstrate that the propagation of epigenetic modifications operates by such a mechanism, it is supported by experimental studies in various model systems, as discussed later.

A number of other mechanisms for chromatin pattern formation in well-mixed systems can be envisioned. One example is Turing patterns that can emerge as self-organizing structures due to different diffusion coefficients of two counteracting enzymes. These have been discussed in the context of biological systems such as pattern formation in animal skin development.⁵⁶ Although Turing patterns could in principle play a role in intracellular pattern formation, they are likely to lack the spatial precision to provide a robust mechanism by which the cell would be able to control the formation of epigenetic chromatin signatures. Loci that are to be modified would have to be positioned rather accurately with respect to each other and with respect to diffusive boundaries to avoid misregulation of gene activity.

Another interesting pattern formation mechanism includes Ising-type models based on nearest-neighbor interactions. Classically, the Ising model was used to describe ferromagnets that contain distinct magnetic domains, but it was also applied to model biological systems such as activity patterns in neural networks.⁵⁷ Recently, models based on nearest-neighbor interactions have also been used to describe epigenetic patterns.^{58,59} In these models, an enzyme preferentially modifies a nucleosome that has a modified neighbor on the same chain, resulting in linear spreading of the modification along the chromosome. Although in simulations these models have been found to produce finite domains around a nucleation site, it seems challenging for the cell to robustly define the position and the size of the domain using a linear-spreading model. In particular, unlimited spreading at the boundary of the domain has to be prevented within the noisy cellular environment, in which protein concentrations and occupancies of binding sites fluctuate. To efficiently realize a nearest-neighbor model on chromatin, the association rate of the modifying enzyme has to be much higher for binding to a modified nucleosome than to a potential substrate. Otherwise, the enzyme could directly modify a substrate nucleosome instead of binding to a modified one and subsequently modifying the neighbor. To our

knowledge, such behavior has not been reported experimentally. Moreover, it is elusive how an enzyme would discriminate between a nucleosome on the same chain and a nucleosome on a different chain if both are located at similar spatial distances in the crowded environment of the nucleus. Thus, it will be interesting to see if a molecular basis for such models will be identified in the future.

Finally, more complex hybrid mechanisms for establishing epigenetic patterns on chromatin were proposed that involve the integration of symmetrical positive-feedback loops in which nucleosomes are actively modified by proteins that bind to a given histone mark and, at the same time, can interact with proteins that set or remove histone modifications.⁶⁰ In the latter model, the enzymes can both act on neighboring nucleosomes and exert some more long-range interactions with nucleosomes at a distance. To limit the spreading of a distinct modification mark, boundary elements were introduced. A similar model was used by Angel *et al.*⁶¹ This type of theoretical description results in bistable chromatin states, that is, for the locus under consideration two distinct states can stably coexist, which could correspond to either transcriptional activity or transcriptional silencing.⁶²

Features of experimentally observed epigenetic patterns

As discussed earlier, confined diffusion of chromatin-bound epigenetic modifiers could give rise to localized finite epigenetic domains. The corresponding modification profiles are expected to follow the intrachromosomal contact probabilities depicted in Figure 2. Thus, a chromosome-bound enzyme would modify nucleosomes on the same chromosome within ~4 kb around its binding site. These expected domain sizes agree very well with experimentally determined histone-methylation profiles, in which the modification was induced by artificially tethering a protein to a specific locus. One example is the recruitment of histone methyltransferase Clr4 to three adjacent *GAL* sites in yeast that results in the histone H3 lysine 9 dimethylation (H3K9me2) profile depicted in Figure 5A.⁶³ In another study, Hathaway *et al.* induced gene silencing by artificially recruiting HP1 in mouse embryonic stem cells and fibroblasts.⁵⁸ They observed spreading of the repressive H3K9me3 modification around the nucleation site with smoothly decreasing bor-

ders (Fig. 5B). In both studies, the histone modification profiles around the locally chromatin-tethered protein were very similar to the local concentration profiles predicted according to Eq. 4 (Fig. 5C). A similarly shaped H3 lysine 27 trimethylation domain was found for the polycomb repressive complex 2 (PRC2)-based silencing of the floral repressor locus C (*FLC*) gene.⁶¹ Thus, the overall shape of histone methylation domains observed in these experiments can be explained as originating from a chromatin-bound enzyme that propagates the modification via chromatin dynamics along the chain. It is noted that the exact size of a domain generated in this manner will also depend on the concentration and activity of the unbound enzyme as well as counteracting enzymes that remove a given histone modification (Fig. 5D–F). In particular, domains will only be formed if the productive collision frequency with immobilized enzymes is significantly higher than modifications catalyzed by the freely diffusive enzymes. In addition to an increase of the local concentration in the vicinity of the chromatin-bound protein, as reflected in the value of j_M , chromatin binding could also involve allosteric activation of the enzyme (e.g., due to multimerization to increase its spatially confined activity). For example, the tethering of the bacterial enhancer-binding protein NtrC to DNA is accompanied by its multimerization to create an active complex that would not form freely in solution and that interacts with RNA polymerase at the promoter through DNA looping.^{64,65} Another potential layer of regulation is the accessibility of the enzymes to different chromatin domains. In case of a significant size difference between a modifying enzyme and its antagonist, densely packed chromatin regions might have a bias for one of the counteracting activities, since only the smaller enzyme can easily access such a region. For example, the histone H3K9 methyltransferases Suv39h1, G9a, GLP, and SETDB1 were found to associate into a complex of MDa molecular weight.⁶⁶ In contrast, a counteracting H3K9me2 demethylation activity for an enzyme from the Jumonji family was present in a complex of only 300 kDa.⁶⁷

The size of the histone modification domain established from a chromatin-bound enzyme is modulated by the frequency of productive collisions of a nucleosome with the counteracting enzyme (Fig. 5E and F). If productive collisions with free modifiers occur rarely and collisions with the

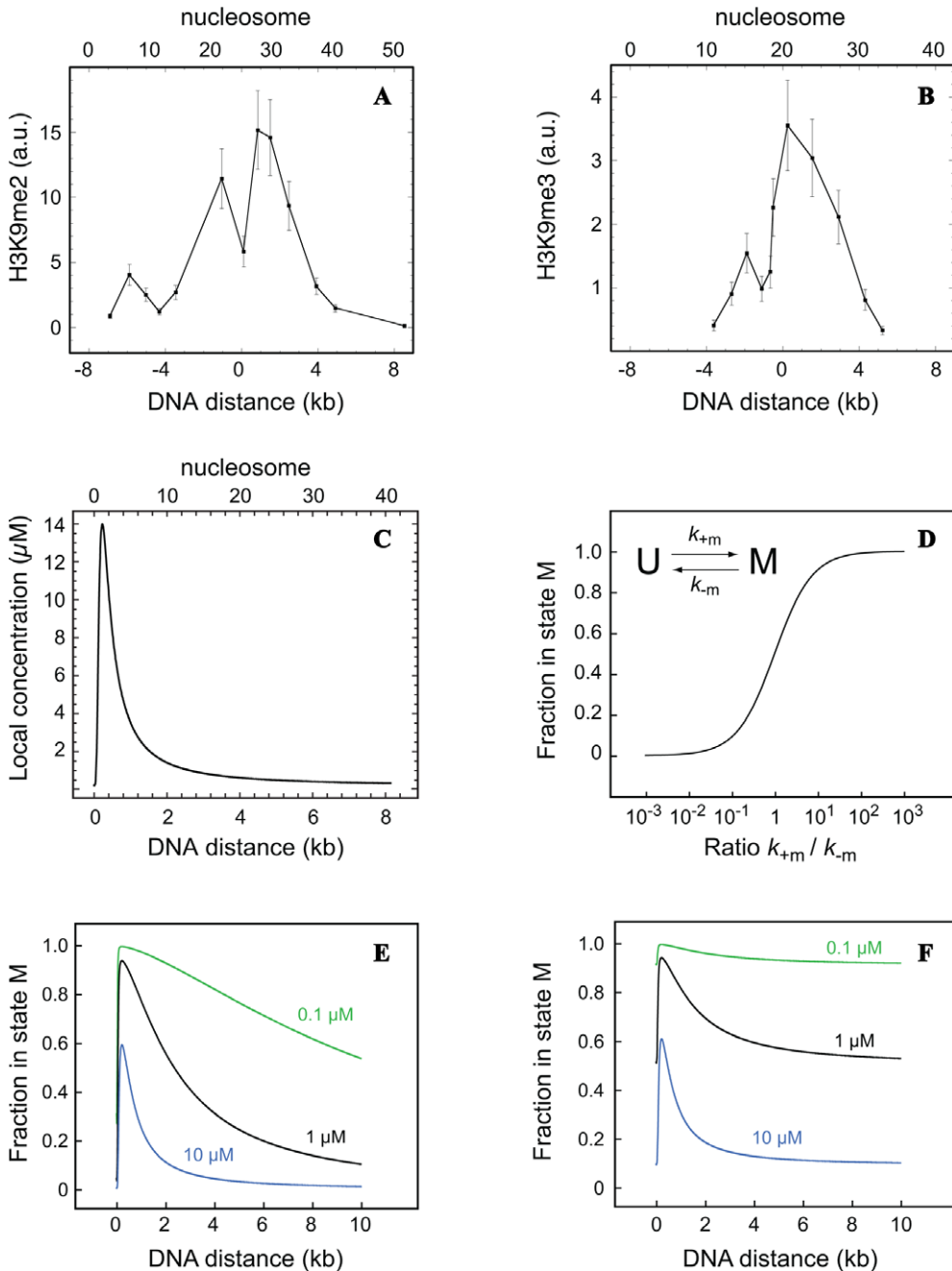


Figure 5. Experimental and theoretical one-dimensional histone modification domain profiles along the nucleosome chain. (A) Artificial recruitment of Clr4, the H3K9-specific methyltransferase in yeast, to three adjacent sites (*GAL* sites) in euchromatin resulted in a symmetrically distributed H3K9 dimethylation profile.⁶³ (B) Artificial tethering of HP1 to a site in the *Oct-4* promoter in mouse cells induced H3K9 trimethylation in the local vicinity.⁵⁸ (C) Calculated local concentrations according to Eq. 4. (D) Histone modifications at a given nucleosome arise from the opposing activities of enzymes that catalyze the addition or removal of the modification M with rates k_{+m} and k_{-m} , respectively, according to the relation $M = 1/(1+k_{-m}/k_{+m}) = k_{+m}/(k_{+m} + k_{-m})$. (E) Histone-modification domains with different spatial extensions can be formed by a mechanism that relies on nucleosomal collisions within the chain. The domain size can be modulated through the concentration and activity of free and bound enzymes. Plots for the indicated concentrations of counteracting soluble enzymes are shown in the absence of free modifying enzyme. (F) Same as in panel E but for a 1 μM concentration of free modifying enzyme.

counteracting enzyme occur more frequently (but less frequently than collisions with the immobilized modifiers), modification profiles that resemble the experimental contact-probability distributions depicted in Figure 5A and B will be obtained. However, for other cases, the relevant parameters might be very different (Fig. 5E and F). If the activity of counteracting processes can be neglected, relatively large domains might be formed. An example for modification domains established in the absence of counteracting processes are the patterns around ectopic *dam* methyltransferase molecules tethered to chromatin or the nuclear lamina. These domains span 2–3 kb on the same chromosome (Fig. 2C) and extend up to 1 μm from the lamina in 3D space.^{31,68} Thus, the cell might be able to establish epigenetic domains up to the 1- μm length scale by adjusting the amount and binding affinity of chromatin-modifying enzymes and their antagonists. The underlying diffusion-driven mechanism simply relies on the intrinsic flexibility of chromatin and does not require additional boundaries to restrict spreading of a given modification. The maximum propagation rate according to this mechanism is limited by the collision frequency between nucleosomes, which is around 1000/s, as described earlier. Most epigenetic modifiers seem to have rather low modification rates, with some minutes for histone acetylation (see Ref. 69 and references therein) and up to hours for histone methylation.⁷⁰ Consistent with this view, the spreading rate measured in living cells for H3K9 trimethylation is rather slow at ~ 0.18 nucleosomes/h.⁵⁸ Thus, the collision frequency between nucleosome substrates and chromatin-bound modifiers does probably not represent a rate-limiting step for epigenetic pattern formation.

Epigenetic memory

A long-standing question in epigenetics is how histone modifications are inherited (i.e., transmitted through genome replication and cell division). For DNA methylation, this is accomplished by a dedicated machinery that recognizes hemi-methylated DNA after replication and reestablishes the fully methylated state.⁷¹ For histone modifications, no comparable duplication mechanism is known and the cell has to cope with the enormous combinatorial variety that arises from at least 80 potential modification sites on histone H3 and H4 that are sub-

ject to acetylation, mono-, di- and trimethylation, phosphorylation, etc. In the model proposed here, histone modifications could simply be transmitted through replication by chromatin-bound enzymes that collide with nucleosomes on both daughter helices (Fig. 1C). This mechanism is compatible with an arbitrary distribution of newly incorporated nucleosomes behind the replication fork, since it is irrelevant on which chain a given modifying enzyme is immobilized. Each chromatin-bound enzyme could establish a modification domain in its spatial proximity via both intra- and interfiber collisions, yielding two fibers with similar patterns. To ensure that the amount of chromatin-bound enzyme is invariant, the density of nucleation sites has to be kept constant. Such nucleation sites could be made up of a specific DNA sequence and/or DNA methylation, which are both retained during replication. In the presence of positive feedback, the propagated histone modification might itself contribute to establish additional nucleation sites. Furthermore, nascent RNA transcripts that originate from a defined locus and bind chromatin-modifying enzymes are candidates for setting up nucleation sites. We find such a simple collision-driven inheritance mechanism very attractive, but note that further experimental investigations are required to demonstrate its existence and molecular details for a given histone modification.

Conclusions

It is a fascinating question how cells manage to establish numerous subcompartments in the nucleus given that diffusion balances concentration gradients of all soluble factors. Since most enzymes that establish localized chromatin states are small enough to diffuse rapidly through the complete cell nucleus, the question arises why epigenetic modifications of nucleosomes and DNA do not display homogeneous distributions that reflect diffusive collisions with the corresponding enzymes within the well-mixed nucleoplasm. Here, we propose a simple mechanism that can explain how epigenetic domains are formed around an enzyme that is bound to chromatin. Random motions of the enzyme together with the chromatin segment to which it is bound will lead to collisions with nucleosomes in spatial proximity and an elevated modification probability in a confined region around the binding site. As described above, many experimental

findings are consistent with such a mechanism for establishing epigenetic patterns. According to our model, the patterns cannot form spontaneously at an arbitrary position but originate from a nucleation site at which the modifying enzyme is immobilized. Nucleation sites might be formed by special sequence elements, modified DNA bases such as 5-methylcytosine, modified histone residues, or chromatin regions with a specific composition of proteins and RNA. Thus, potential patterns would be imprinted in the chromatin polymer as a distribution of these nucleation sites, which can be bound and interpreted if the appropriate adaptor molecules are present. On the one hand, this ensures robustness, since patterns cannot emerge spontaneously at the wrong sites and cannot extend erroneously into regions where they should not be. On the other hand, the activation of imprinted nucleation sites depends on macromolecules that bind them, that is, patterns can be switched by modulating the expression level, the intracellular localization, or the binding behavior of these molecules. Upon some stimulus, the cell can bring the appropriate adaptor molecule into the nucleus, which then leads to the activation of the respective nucleation sites and the formation of a given epigenetic pattern. An example would be a hormone receptor that is imported into the nucleus upon hormone exposure. Thus, a rather static distribution of nucleation sites that is stably imprinted into chromatin of a given cell type can be interpreted in a dynamic fashion to endow the cell with sufficient plasticity.

The formation of extended epigenetic patterns as opposed to the modulation of single genes might be beneficial for the cell to increase the robustness of gene regulation. First, genes that are located in spatial proximity can easily be coregulated, which introduces some kind of modularity into the collection of gene expression programs. If genes were targeted individually, all binding affinities at their regulatory sequences would have to be the same to ensure equal dose–response curves, and stochastic effects that could arise from low numbers of activators binding only to a subset of target genes would become critical. Second, single mutations in binding sites could lead to complete deregulation of a particular gene but would not abolish the formation of a local epigenetic pattern if a redundant subset of nucleation sites was present. This might enhance cellular tolerance with respect to mutations. Third, a

memory effect is achieved if a histone modification with low turnover is established, i.e., gene expression can be regulated on the desired time scale independently of the duration of a given stimulus. This is useful for modulating the strength of responses to transient stimuli.

The local propagation mechanism described here is not limited to linear progression along a chromatin fiber but happens in three dimensions, since there is no preferred direction of the diffusive motion of the nucleosome chain. Accordingly, it provides a straightforward explanation for the approximately spherical shape of macroscopic modification patterns.^{72,73} This is different from models that either involve a linear-spreading mechanism along the DNA that exclusively targets residues adjacent to methylated ones which can be modified^{58,59} or that implicitly involve a looping of the nucleosome chain to allow for interaction between distant regions but invoke the existence of so-called boundary or insulator elements to limit spreading.⁶⁰ The mechanism described here has a simple molecular basis and might be applicable to many cellular processes. Furthermore, from an evolutionary point of view it seems simpler to develop a patterning mechanism that relies on the intrinsic flexibility of chromatin compared to the coevolution of additional mechanisms that are responsible for positioning boundaries. Thus, we anticipate that patterning mechanisms driven by the localized propagation of epigenetic marks via chromatin dynamics and bound modifiers will prove to be relevant for our understanding of chromatin biology.

Acknowledgments

K.R. is grateful to the organizers of the workshop “Evolutionary Dynamics and Information Hierarchies” that was held on August 19–September 9, 2012 at the Aspen Center for Physics in Aspen, Colorado, where part of this work was conducted. Furthermore, we thank Katharina Deeg for critically reading the manuscript and Vladimir Teif and Thomas Höfer for discussion, and acknowledge support within the project *EpiSys* by the German Federal Ministry of Education and Research (BMBF) in the SysTec program.

Conflicts of interest

The authors declare no conflicts of interest.

References

- Grewal, S.I. & S. Jia. 2007. Heterochromatin revisited. *Nat. Rev. Genet.* **8**: 35–46.
- Eissenberg, J.C. & G. Reuter. 2009. Cellular mechanism for targeting heterochromatin formation in *Drosophila*. *Int. Rev. Cell Mol. Biol.* **273**: 1–47.
- Allshire, R.C. & G.H. Karpen. 2008. Epigenetic regulation of centromeric chromatin: old dogs, new tricks? *Nat. Rev. Genet.* **9**: 923–937.
- Black, B.E. & D.W. Cleveland. 2011. Epigenetic centromere propagation and the nature of CENP-a nucleosomes. *Cell* **144**: 471–479.
- Probst, A.V. & G. Almouzni. 2008. Pericentric heterochromatin: dynamic organization during early development in mammals. *Differentiation* **76**: 15–23.
- Maison, C. *et al.* 2010. Heterochromatin at mouse pericentromeres: a model for de novo heterochromatin formation and duplication during replication. *Cold Spring Harbor Symp. Quant. Biol.* **75**: 155–165.
- Blasco, M.A. 2007. The epigenetic regulation of mammalian telomeres. *Nat. Rev. Genet.* **8**: 299–309.
- de Lange, T., V. Lundblad & E. Blackburn. 2006. *Telomeres*. Cold Spring Harbor: Cold Spring Harbor Laboratory Press.
- Grummt, I. & G. Langst. 2013. Epigenetic control of RNA polymerase I transcription in mammalian cells. *Biochim. Biophys. Acta.* **1829**: 393–404.
- Filion, G.J. *et al.* 2010. Systematic protein location mapping reveals five principal chromatin types in *Drosophila* cells. *Cell* **143**: 212–224.
- Kharchenko, P.V. *et al.* 2011. Comprehensive analysis of the chromatin landscape in *Drosophila melanogaster*. *Nature* **471**: 480–485.
- Ernst, J. *et al.* 2011. Mapping and analysis of chromatin state dynamics in nine human cell types. *Nature* **473**: 43–49.
- Shogren-Knaak, M. *et al.* 2006. Histone H4-K16 acetylation controls chromatin structure and protein interactions. *Science* **311**: 844–847.
- Robinson, P.J.J. *et al.* 2008. 30 nm chromatin fibre decompaction requires both H4-K16 acetylation and linker histone eviction. *J. Mol. Biol.* **381**: 816–825.
- Daujat, S. *et al.* 2009. H3K64 trimethylation marks heterochromatin and is dynamically remodeled during developmental reprogramming. *Nat. Struct. Mol. Biol.* **16**: 777–781.
- Watanabe, S. *et al.* 2013. A histone acetylation switch regulates H2A.Z deposition by the SWR-C remodeling enzyme. *Science* **340**: 195–199.
- Yang, D. & G. Arya. 2011. Structure and binding of the H4 histone tail and the effects of lysine 16 acetylation. *Phys. Chem. Chem. Phys.* **13**: 2911–2921.
- Allahverdi, A. *et al.* 2011. The effects of histone H4 tail acetylations on cation-induced chromatin folding and self-association. *Nucleic Acids Res.* **39**: 1680–1691.
- Adkins, N.L. & P.T. Georgel. 2011. MeCP2: structure and function. *Biochem. Cell Biol.* **89**: 1–11.
- Thiru, A. *et al.* 2004. Structural basis of HP1/PXVXL motif peptide interactions and HP1 localisation to heterochromatin. *EMBO J.* **23**: 489–499.
- Erdel, F. *et al.* 2011. Targeting chromatin remodelers: signals and search mechanisms. *Biochim. Biophys. Acta.* **1809**: 497–508.
- Teif, V.B. *et al.* 2012. Genome-wide nucleosome positioning during embryonic stem cell development. *Nat. Struct. Mol. Biol.* **19**: 1185–1191.
- Rippe, K., P.H. von Hippel & J. Langowski. 1995. Action at a distance: DNA-looping and initiation of transcription. *Trends Biochem. Sci.* **20**: 500–506.
- Rippe, K. 2001. Making contacts on a nucleic acid polymer. *Trends Biochem. Sci.* **26**: 733–740.
- Cremer, T. & M. Cremer. 2010. Chromosome territories. *Cold Spring Harbor Perspect. Biol.* **2**: a003889.
- Strickfaden, H., T. Cremer & K. Rippe. 2012. “Higher order chromatin organization and dynamics.” In *Genome Organization and Function in the Cell Nucleus*. K. Rippe, Ed.: 417–447. Weinheim: Wiley-VCH.
- Jegou, T. *et al.* 2009. Dynamics of telomeres and promyelocytic leukemia nuclear bodies in a telomerase negative human cell line. *Mol. Biol. Cell.* **20**: 2070–2082.
- Levi, V. *et al.* 2005. Chromatin dynamics in interphase cells revealed by tracking in a two-photon excitation microscope. *Biophys. J.* **89**: 4275–4285.
- Hihara, S. *et al.* 2012. Local nucleosome dynamics facilitate chromatin accessibility in living mammalian cells. *Cell Rep.* **2**: 1645–1656.
- Dekker, J., M.A. Marti-Renom & L.A. Mirny. 2013. Exploring the three-dimensional organization of genomes: interpreting chromatin interaction data. *Nat. Rev. Genet.* **14**: 390–403.
- van Steensel, B. & S. Henikoff. 2000. Identification of *in vivo* DNA targets of chromatin proteins using tethered dam methyltransferase. *Nat. Biotechnol.* **18**: 424–428.
- Ringrose, L. *et al.* 1999. Quantitative comparison of DNA looping *in vitro* and *in vivo*: chromatin increases effective DNA flexibility at short distances. *EMBO J.* **18**: 6630–6641.
- Dostie, J. *et al.* 2006. Chromosome Conformation Capture Carbon Copy (5C): a massively parallel solution for mapping interactions between genomic elements. *Genome Res.* **16**: 1299–1309.
- Dixon, J.R. *et al.* 2012. Topological domains in mammalian genomes identified by analysis of chromatin interactions. *Nature* **485**: 376–380.
- Kuhn, W. 1934. Über die Gestalt fadenförmiger Moleküle in Lösungen. *Koll. Z.* **68**: 2–15.
- Jacobson, H. & W.H. Stockmayer. 1950. Intramolecular reaction in polycondensations. I. The theory of linear systems. *J. Chem. Phys.* **18**: 1600–1606.
- Flory, P.J. 1969. *Statistical Mechanics of Chain Molecules*. New York: Wiley.
- Kratky, O. & G. Porod. 1949. Röntgenuntersuchung gelöster Fadenmoleküle. *Rec. Trav. Chim.* **68**: 1106–1113.
- Shimada, J. & H. Yamakawa. 1984. Ring-closure probabilities of twisted wormlike chains. Application to DNA. *Macromolecules* **17**: 689–698.
- Becker, N.B., A. Rosa & R. Everaers. 2010. The radial distribution function of worm-like chains. *Eur. Phys. J. E. Soft Matter.* **32**: 53–69.

41. Merlitz, H. *et al.* 1998. Looping dynamics of linear DNA molecules and the effect of DNA curvature: a study by Brownian dynamics simulation. *Biophys. J.* **74**: 773–779.
42. Rippe, K. 2012. “The folding of the nucleosome chain.” In *Genome Organization and Function in the Cell Nucleus*. K. Rippe, Ed.: 139–167. Weinheim: Wiley-VCH.
43. Rippe, K., R. Stehr & G. Wedemann. 2012. “Monte Carlo simulations of nucleosome chains to identify factors that control DNA compaction and access.” In *Innovations in Biomolecular Modeling and Simulation*. T. Schlick, Ed.: 198–235. Cambridge: RSC Publishing.
44. Kulaeva, O.I. *et al.* 2012. Internucleosomal interactions mediated by histone tails allow distant communication in chromatin. *J. Biol. Chem.* **287**: 20248–20257.
45. Kepper, N. *et al.* 2011. Force spectroscopy of chromatin fibers: extracting energetics and structural information from Monte Carlo simulations. *Biopolymers* **95**: 435–447.
46. Bonnet, G., O. Krichevsky & A. Libchaber. 1998. Kinetics of conformational fluctuations in DNA hairpin-loops. *Proc. Natl. Acad. Sci. USA* **95**: 8602–8606.
47. Cremer, T. & C. Cremer. 2001. Chromosome territories, nuclear architecture and gene regulation in mammalian cells. *Nat. Rev. Genet.* **2**: 292–301.
48. Weidemann, T. *et al.* 2003. Counting nucleosomes in living cells with a combination of fluorescence correlation spectroscopy and confocal imaging. *J. Mol. Biol.* **334**: 229–240.
49. Crick, F. 1970. Diffusion in embryogenesis. *Nature* **225**: 420–422.
50. Yu, S.R. *et al.* 2009. Fgf8 morphogen gradient forms by a source-sink mechanism with freely diffusing molecules. *Nature* **461**: 533–536.
51. Driever, W. & C. Nusslein-Volhard. 1988. A gradient of bicoid protein in *Drosophila* embryos. *Cell* **54**: 83–93.
52. Carazo-Salas, R.E. *et al.* 1999. Generation of GTP-bound Ran by RCC1 is required for chromatin-induced mitotic spindle formation. *Nature* **400**: 178–181.
53. Nemergut, M.E. *et al.* 2001. Chromatin docking and exchange activity enhancement of RCC1 by histones H2A and H2B. *Science* **292**: 1540–1543.
54. Klebe, C. *et al.* 1995. Interaction of the nuclear GTP-binding protein Ran with its regulatory proteins RCC1 and RanGAP1. *Biochemistry* **34**: 639–647.
55. Hinkle, B. *et al.* 2002. Chromosomal association of Ran during meiotic and mitotic divisions. *J. Cell Sci.* **115**: 4685–4693.
56. Maini, P.K., R.E. Baker & C.M. Chuong. 2006. Developmental biology. The Turing model comes of molecular age. *Science* **314**: 1397–1398.
57. Hopfield, J.J. 1982. Neural networks and physical systems with emergent collective computational abilities. *Proc. Natl. Acad. Sci. USA* **79**: 2554–2558.
58. Hathaway, N.A. *et al.* 2012. Dynamics and memory of heterochromatin in living cells. *Cell* **149**: 1447–1460.
59. Hodges, C. & G.R. Crabtree. 2012. Dynamics of inherently bounded histone modification domains. *Proc. Natl. Acad. Sci. U. S. A.* **109**: 13296–13301.
60. Dodd, I.B. *et al.* 2007. Theoretical analysis of epigenetic cell memory by nucleosome modification. *Cell* **129**: 813–822.
61. Angel, A. *et al.* 2011. A Polycomb-based switch underlying quantitative epigenetic memory. *Nature* **476**: 105–108.
62. Ferrell, J.E. 2012. Bistability, bifurcations, and Waddington’s epigenetic landscape. *Curr. Biol.* **22**: R458–R466.
63. Kagansky, A. *et al.* 2009. Synthetic heterochromatin bypasses RNAi and centromeric repeats to establish functional centromeres. *Science* **324**: 1716–1719.
64. Rippe, K., N. Mücke & A. Schulz. 1998. Association states of the transcription activator protein NtrC from *E. coli* determined by analytical ultracentrifugation. *J. Mol. Biol.* **278**: 915–933.
65. Schulz, A., J. Langowski & K. Rippe. 2000. The effect of the DNA conformation on the rate of NtrC activated transcription of *E. coli* RNA Polymerase ^{s54} holoenzyme. *J. Mol. Biol.* **300**: 709–725.
66. Fritsch, L. *et al.* 2010. A subset of the histone H3 lysine 9 methyltransferases Suv39h1, G9a, GLP, and SETDB1 participate in a multimeric complex. *Mol. Cell* **37**: 46–56.
67. Yamane, K. *et al.* 2006. JHDM2A, a JmjC-containing H3K9 demethylase, facilitates transcription activation by androgen receptor. *Cell* **125**: 483–495.
68. Kind, J. *et al.* 2013. Single-cell dynamics of genome-nuclear lamina interactions. *Cell* **153**: 178–192.
69. Görisch, S.M. *et al.* 2005. Histone acetylation increases chromatin accessibility. *J. Cell Sci.* **118**: 5825–5834.
70. Zee, B.M. *et al.* 2010. *In vivo* residue-specific histone methylation dynamics. *J. Biol. Chem.* **285**: 3341–3350.
71. Law, J.A. & S.E. Jacobsen. 2010. Establishing, maintaining and modifying DNA methylation patterns in plants and animals. *Nat. Rev. Genet.* **11**: 204–220.
72. Bewersdorf, J., B.T. Bennett & K.L. Knight. 2006. H2AX chromatin structures and their response to DNA damage revealed by 4Pi microscopy. *Proc. Natl. Acad. Sci. USA* **103**: 18137–18142.
73. Eck, S. *et al.* 2013. Segmentation of heterochromatin foci using a 3D spherical harmonics intensity model. In *Bildverarbeitung für die Medizin 2013*, H.-P. Meinzer *et al.*, Eds.: 308–313. Berlin: Springer.